Supporting Information

Reasonable regulation of flexible sulfur based bifunctional catalytic electrodes for efficient seawater splitting

Fengjing Lei[#a], Xunwei Ma[#b], XinYun Shao[a], Ziyan Fang[a], Yuqin Wang[a], Weiju Hao*[a]

[a]School of Materials and Chemistry, University of Shanghai for Science and Technology, Shanghai 200093, P. R. China.

[b]School of Resource and Environmental Engineering, Shanghai Polytechnic University, Shanghai 201209, P. R.

[#] The authors are equal to this work.

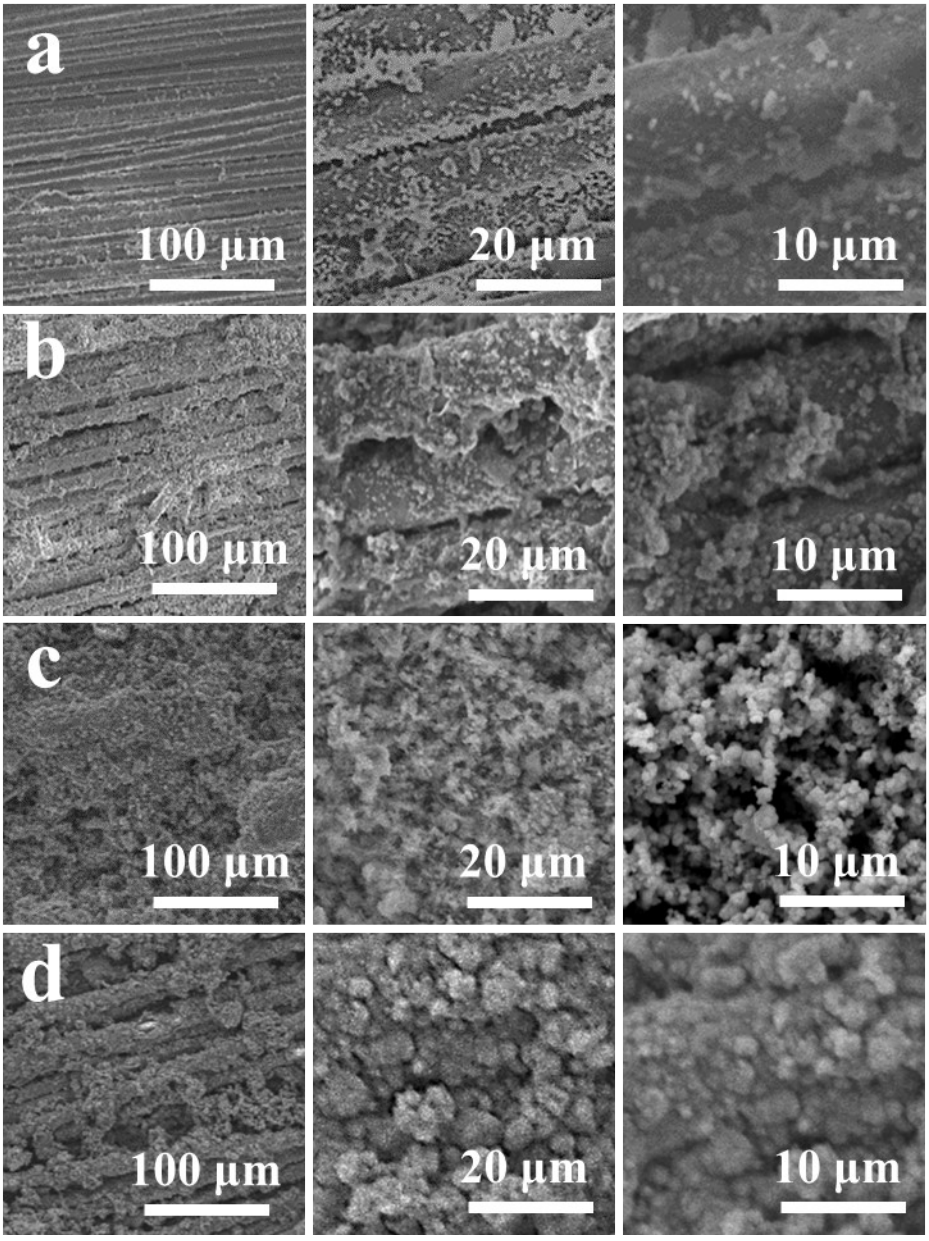

Fig. S1 SEM images of (a) Fe-NiS@HA 3 h; (b) Fe-NiS@HA 6 h; (c) Fe-NiS@HA 12 h and (d) Fe-NiS@HA 24 h with different magnification.

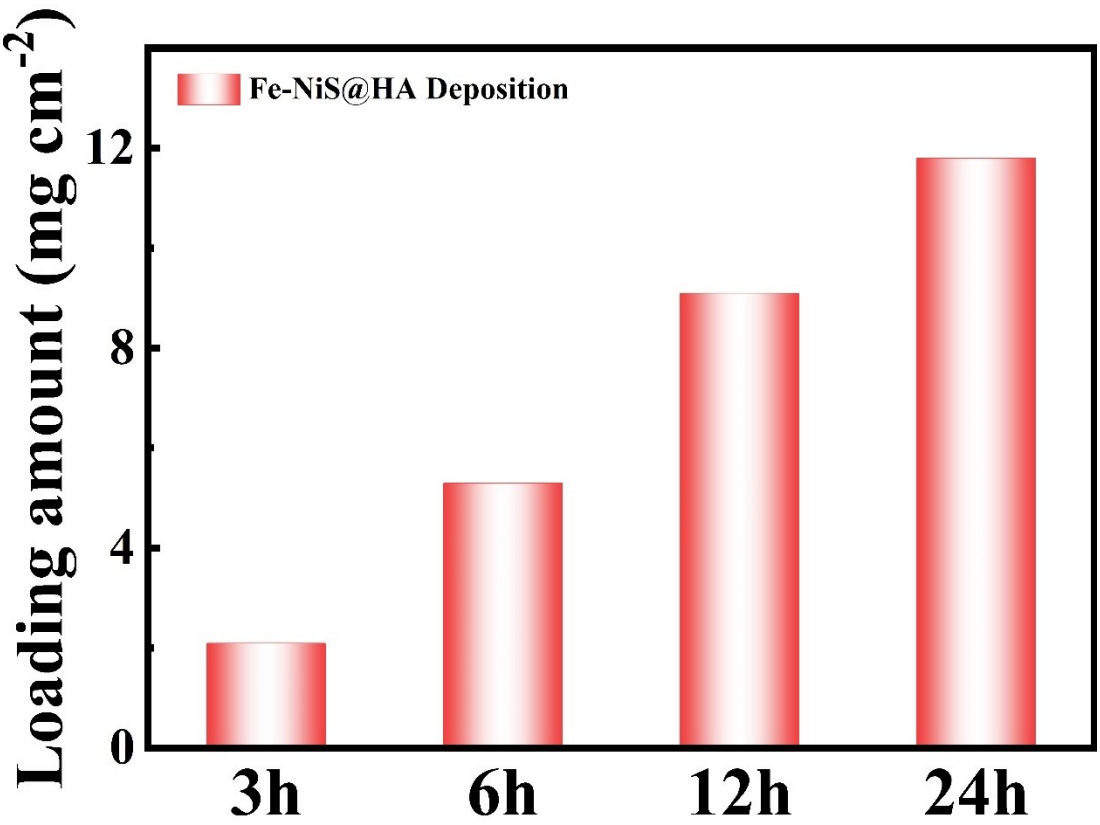

Fig. S2 Loading amount of Fe-NiS@HA with different electroless plating (EP) time.

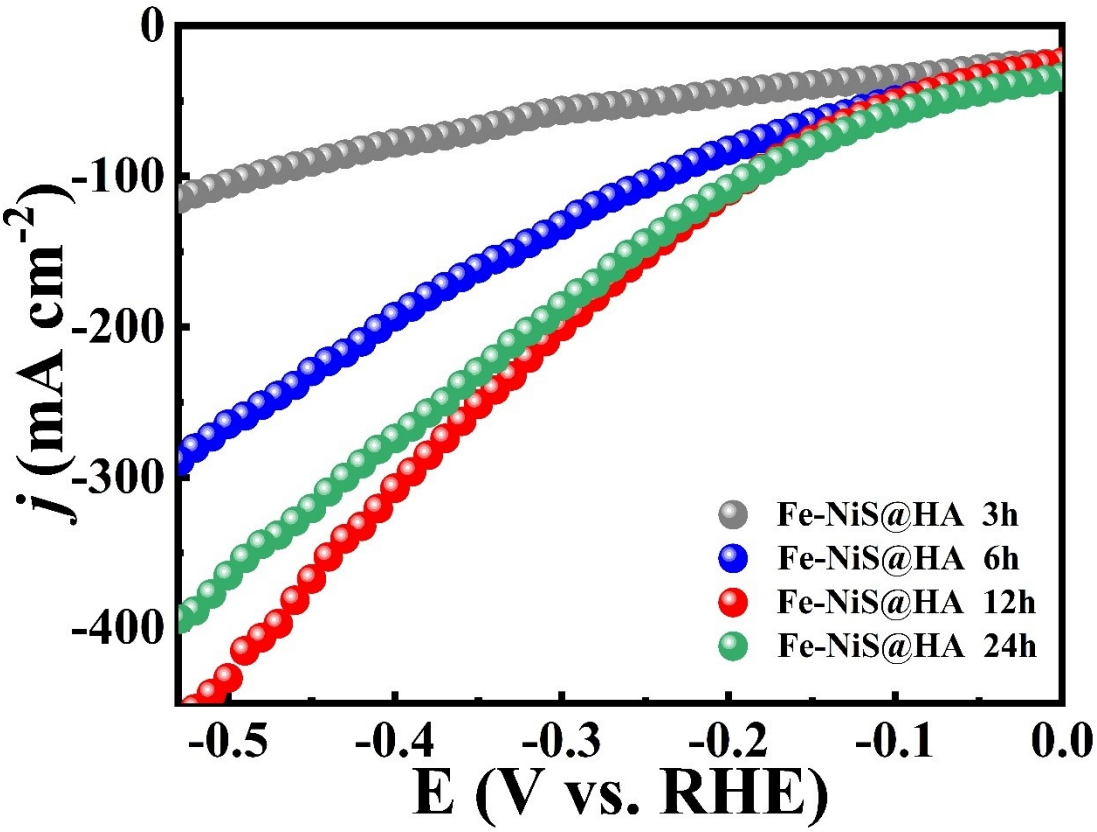

Fig. S3 *iR*-uncorrected LSV curves of Fe-NiS@HA with different electroless plating (EP) time during HER process.

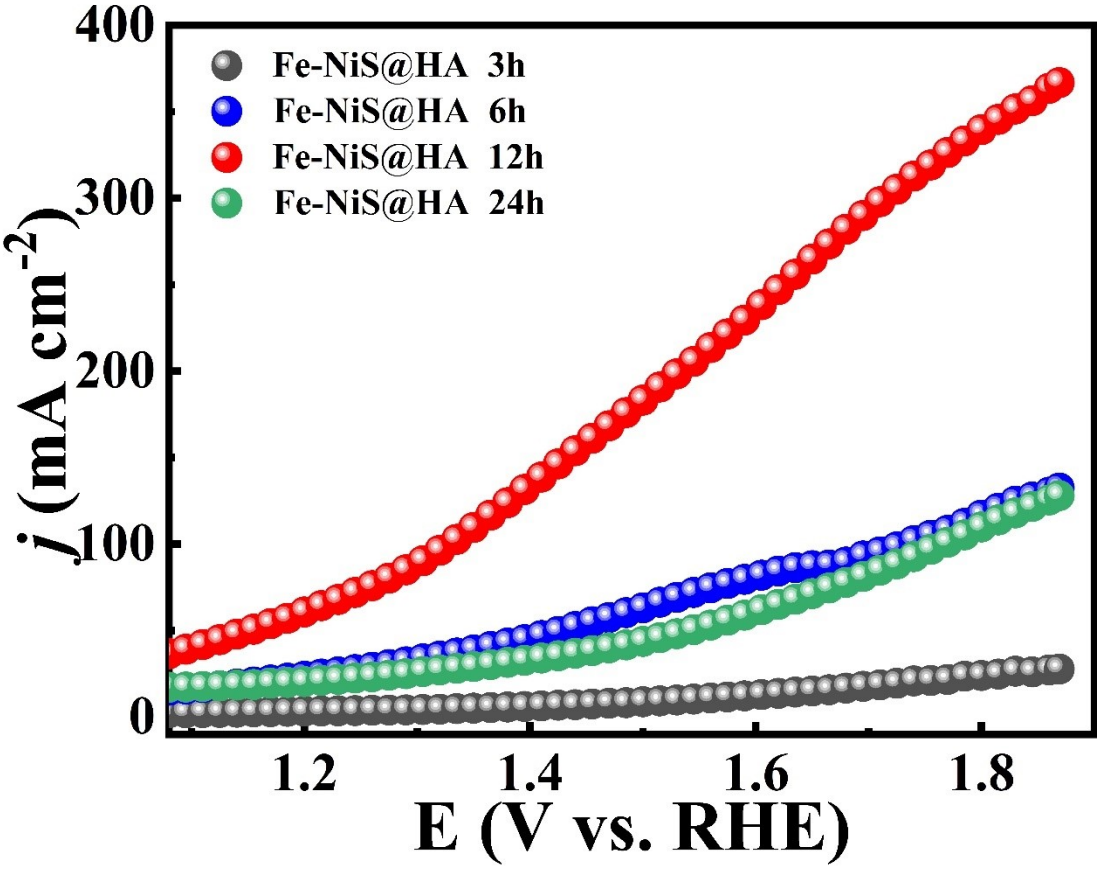

Fig. S4 iR-uncorrected LSV curves of Fe-NiS@HA with different electroless plating (EP) time during OER process.

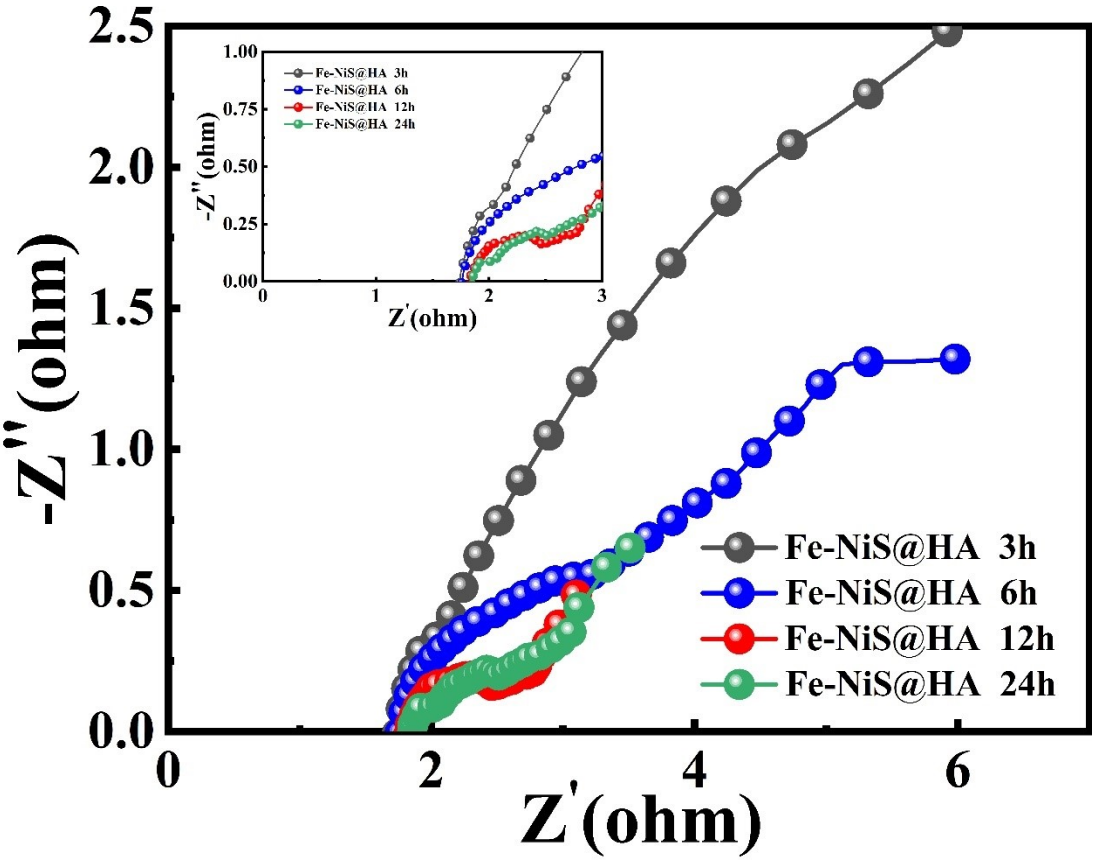

Fig. S5 Nyquist plots derived from EIS measurements of Fe-NiS@HA with different electroless plating (EP) time during HER process.

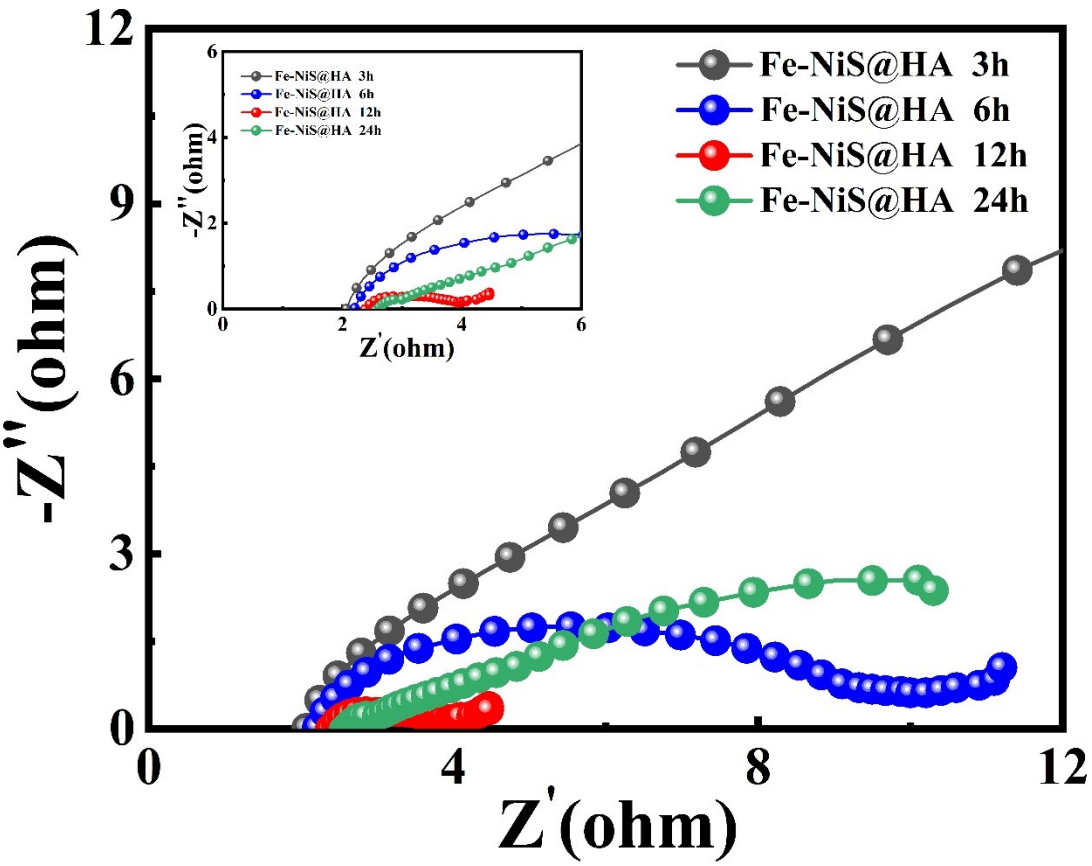

Fig. S6 Nyquist plots derived from EIS measurements of Fe-NiS@HA with different electroless plating (EP) time during OER process.

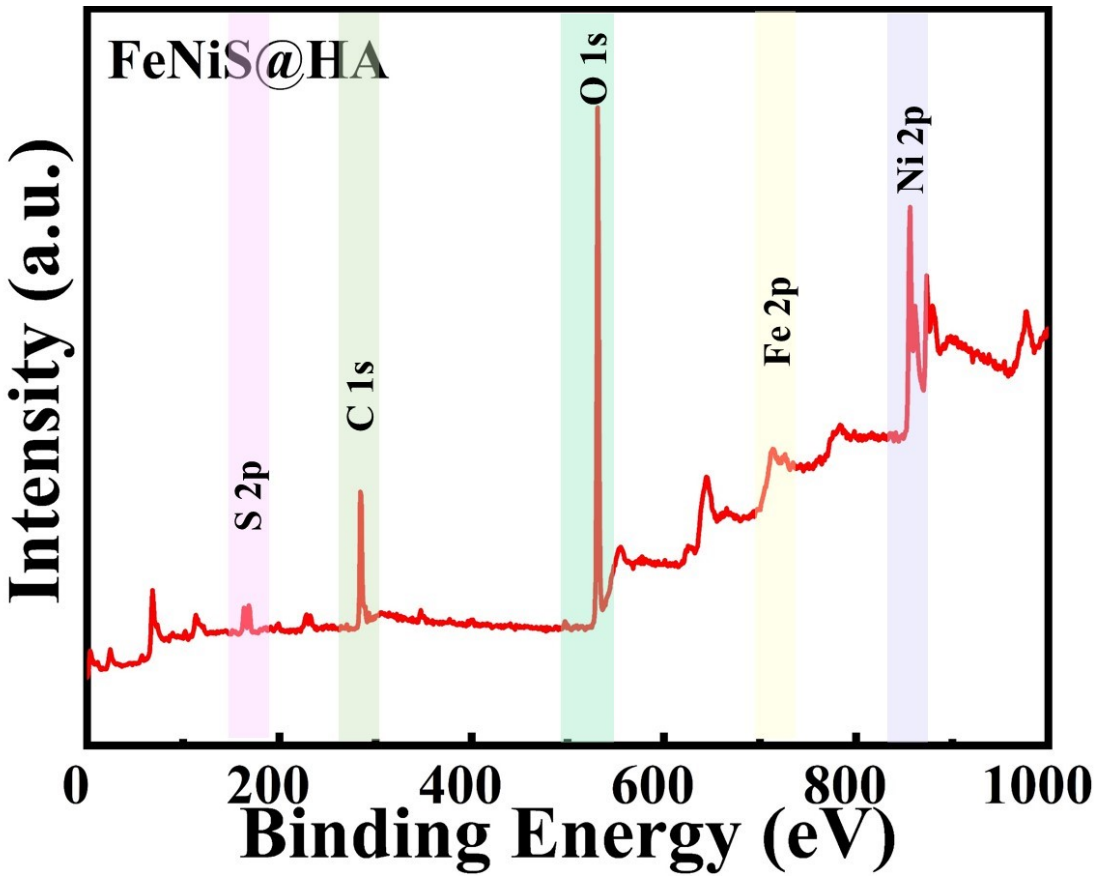

Fig.S7 High-resolution X-ray photoelectron spectroscopy spectrum of full for Fe-NiS@HA.

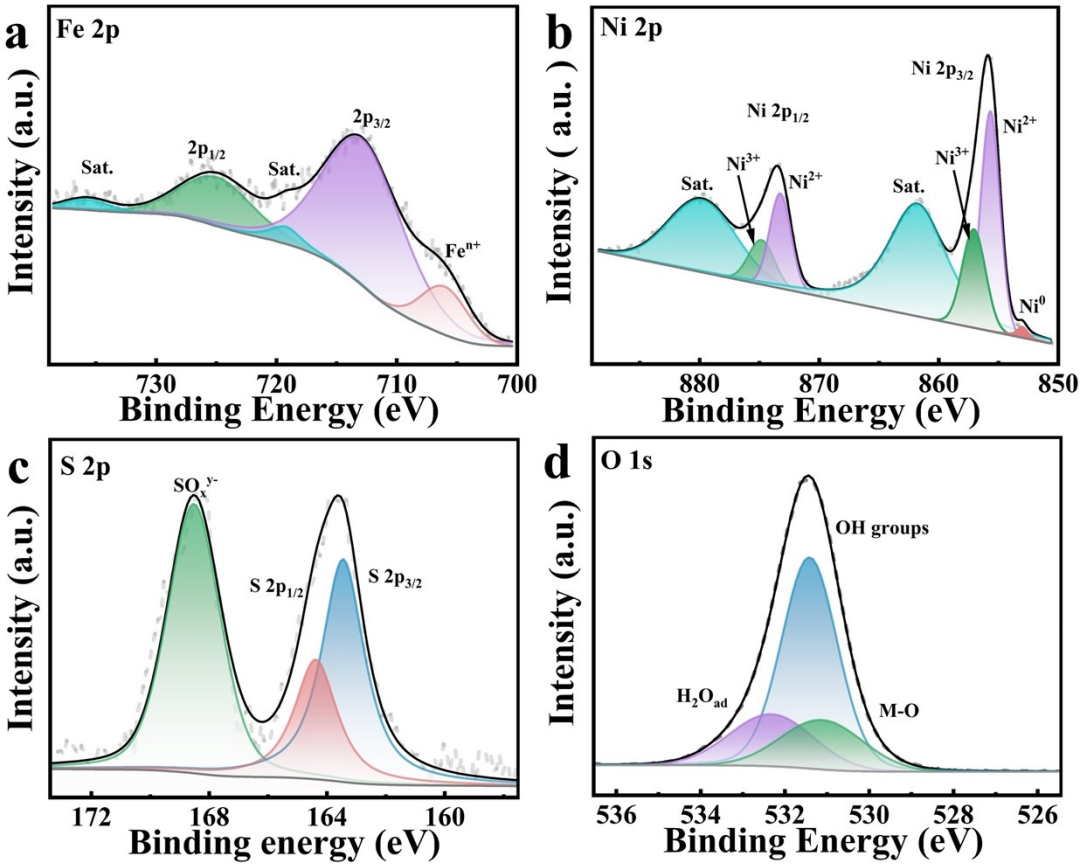

Fig. S8 High resolution XPS spectrum of (a) Fe 2p, (b) Ni 2p, (c) S 2p and (d) O 1s.

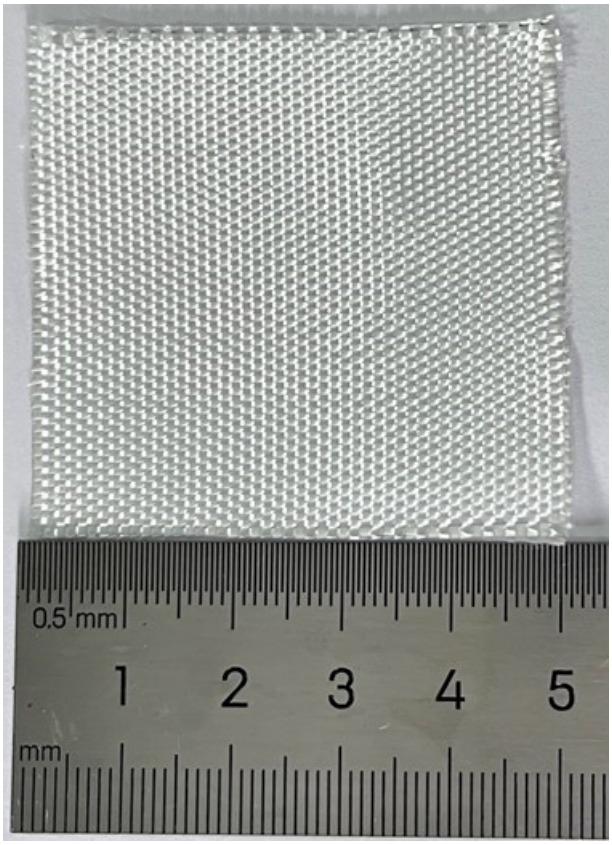

Fig. S9 Bare HA is observed in the macroscopic scale.

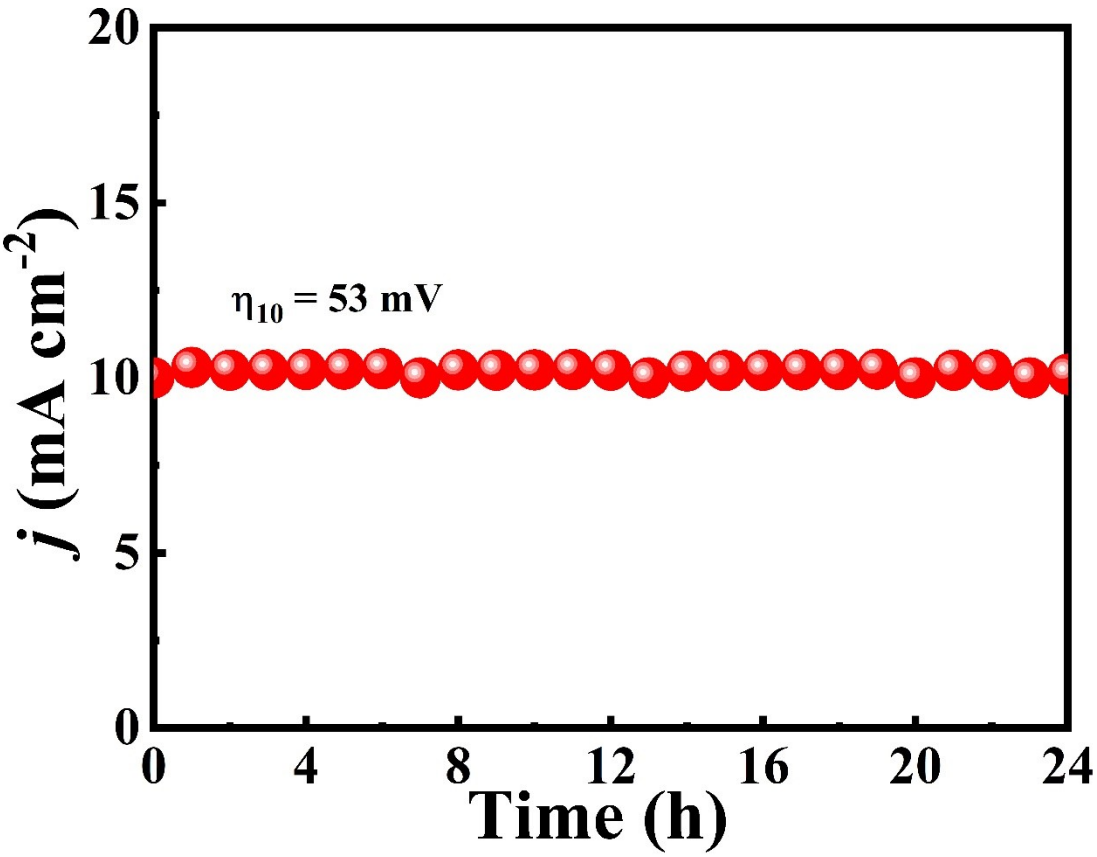

Fig. S10 Chronopotentiometry (*j*-*t*) curve of Fe-NiS@HA for HER at 10 m A cm^{-2}.

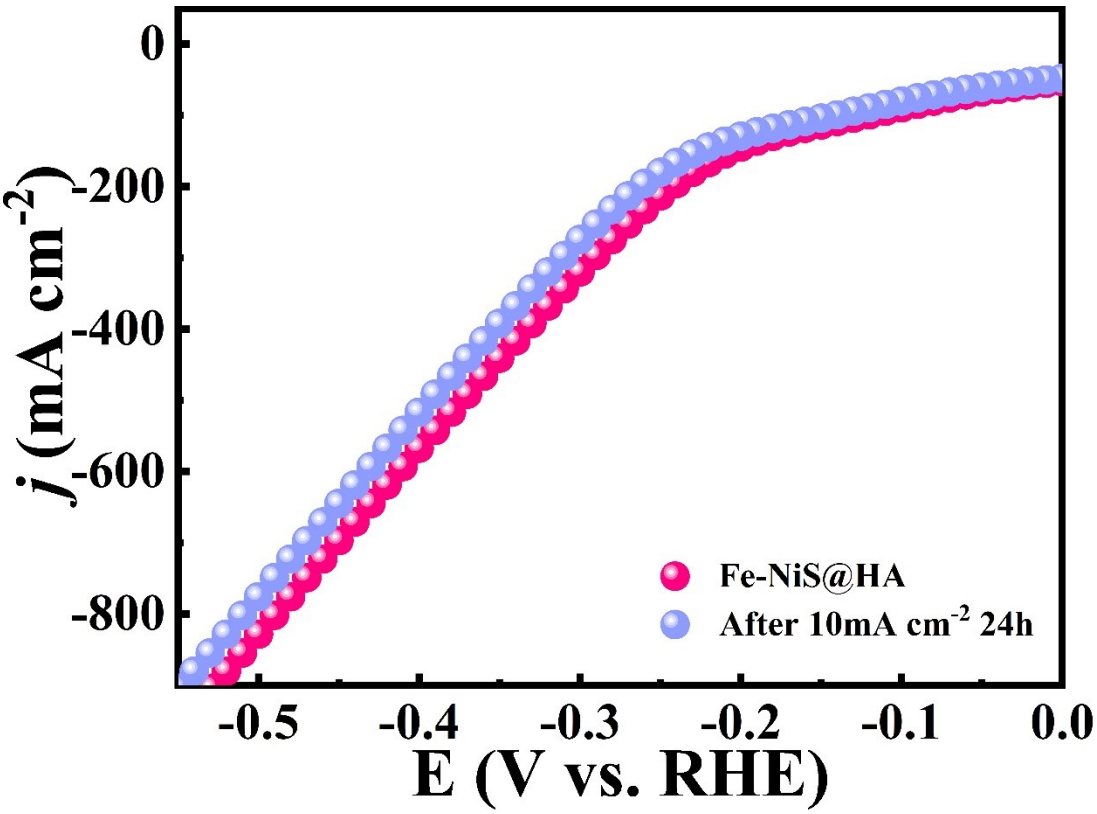

Fig. S11 LSV curves of Fe-NiS@HA before and after 24 h chronoamperometric response for HER at 10 mA cm^{-2}.

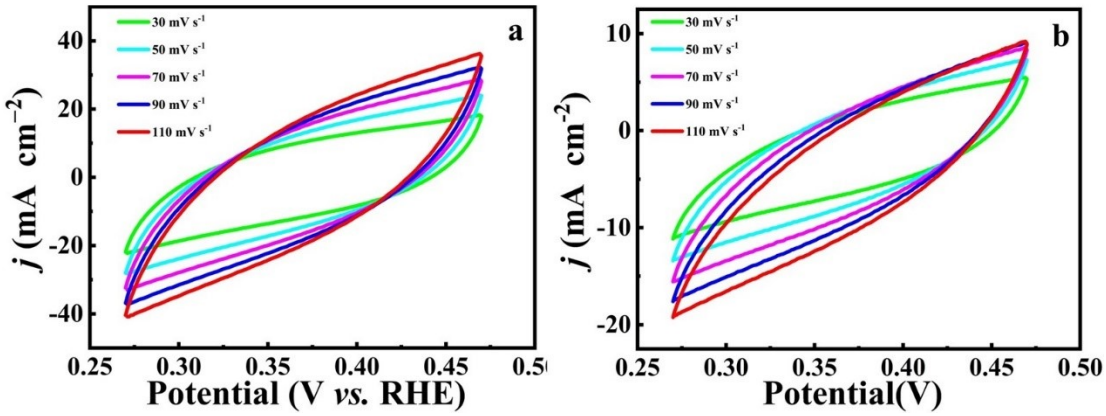

Fig. S12 CV curves within a non-faradaic reaction region of 0.25 ~ 0.5 V (vs. RHE) at different scan rates toward HER for Fe-NiS@HA(a) and NiS@HA(b)

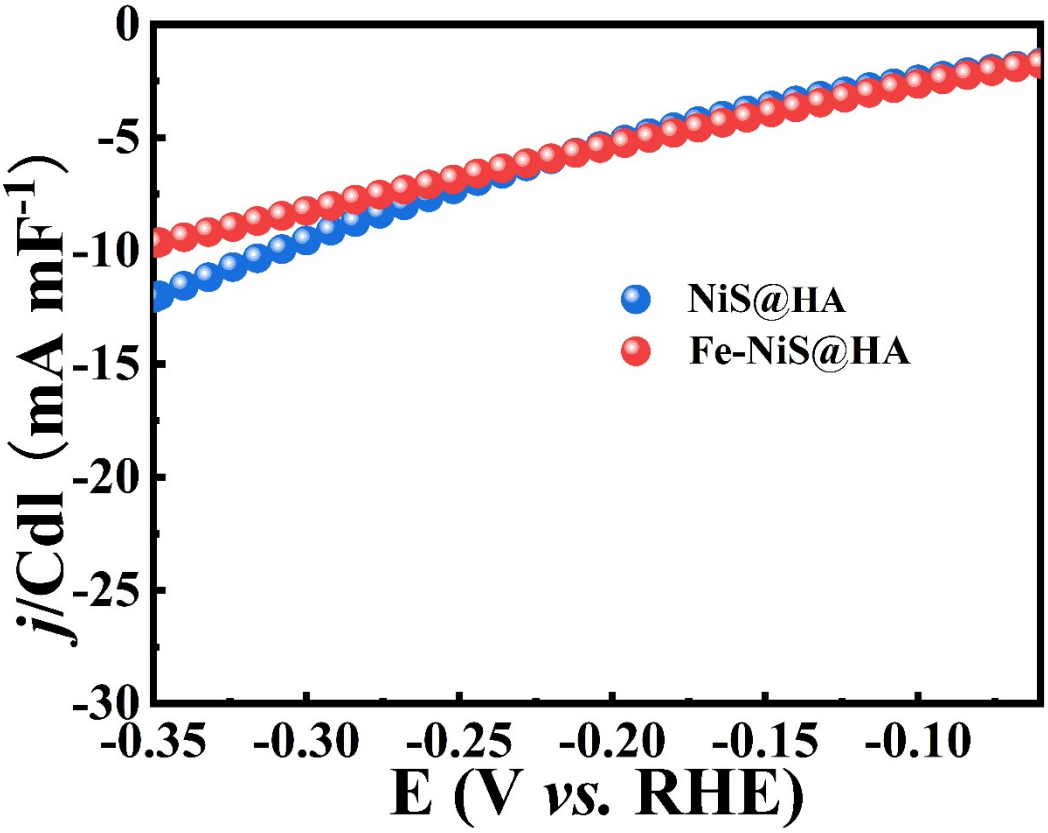

Fig. S13 C_{dl}-normalized LSV curves of Fe-NiS@HA and NiS@HA for HER.

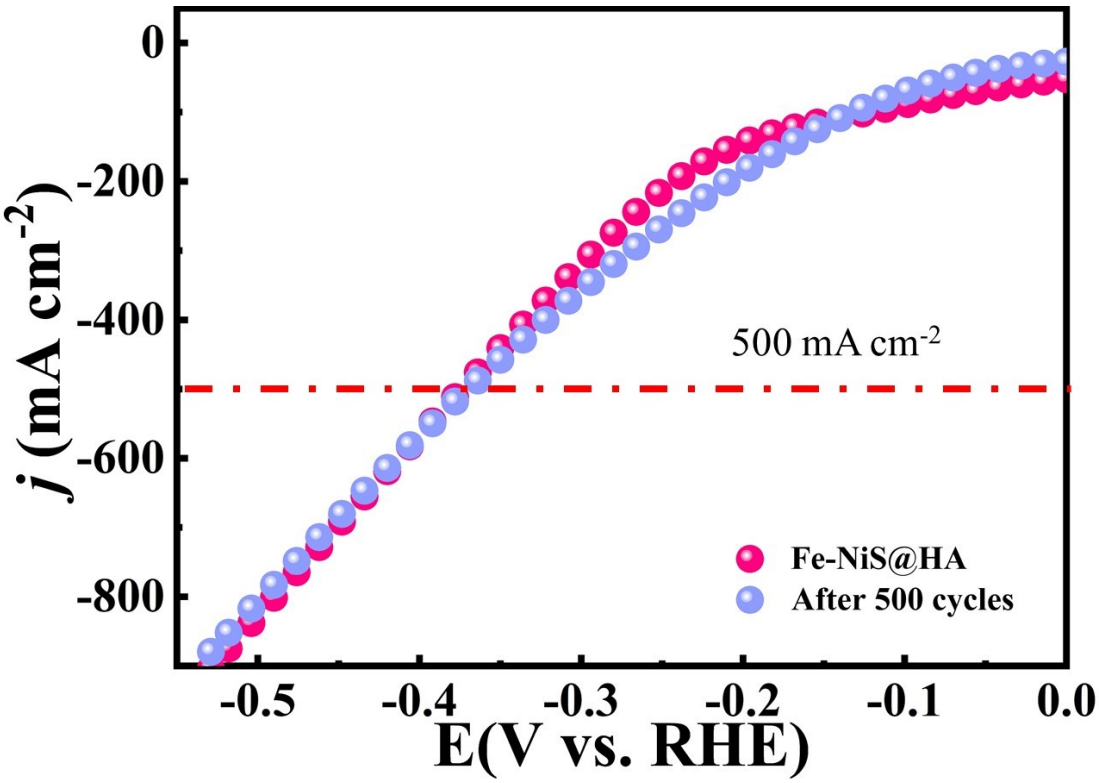

Fig. S14 LSV curves of Fe-NiS@HA before and after 500 HER cycles.

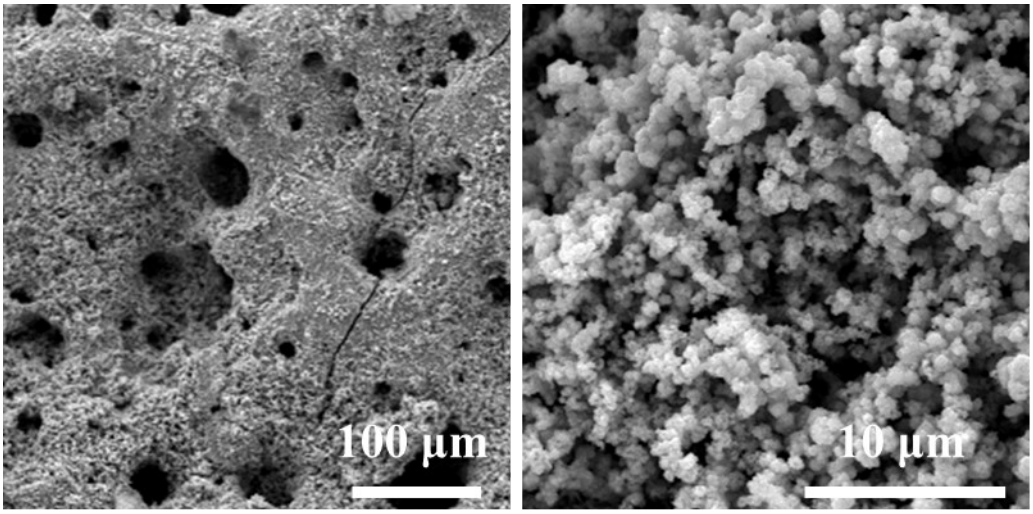

Fig. S15 SEM images of Fe-NiS@HA after HER stability test.

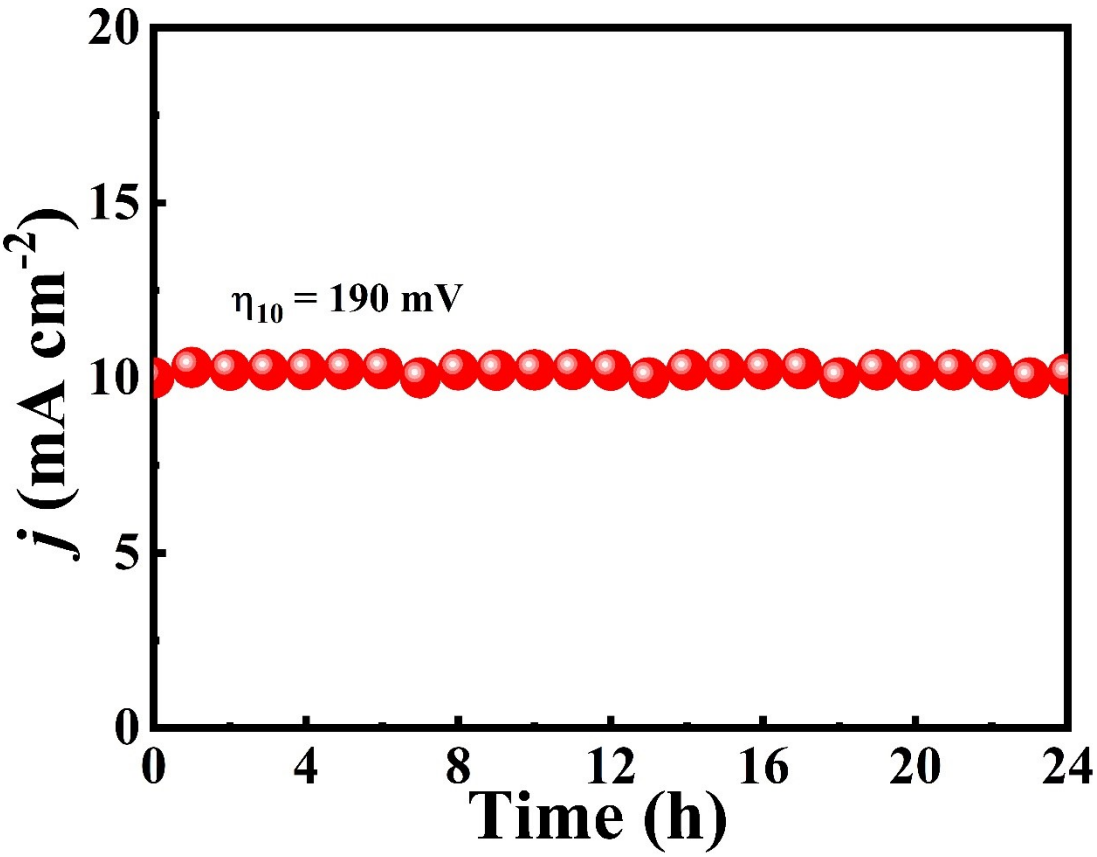

Fig. S16 Chronopotentiometry (j-t) curve of Fe-NiS@HA for OER at 10 m A cm^{-2}.

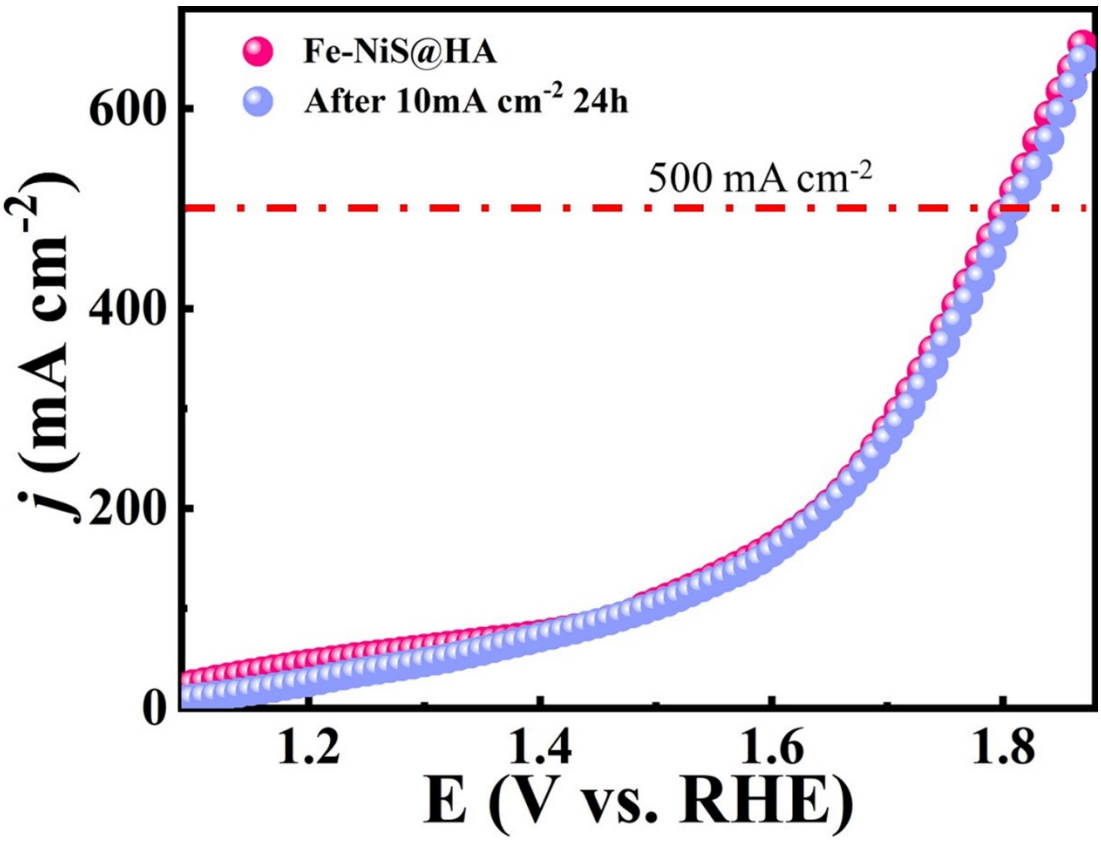

Fig. S17 LSV curves of Fe-NiS@HA before and after 24 h chronoamperometric response for OER at 10 mA cm^{-2}.

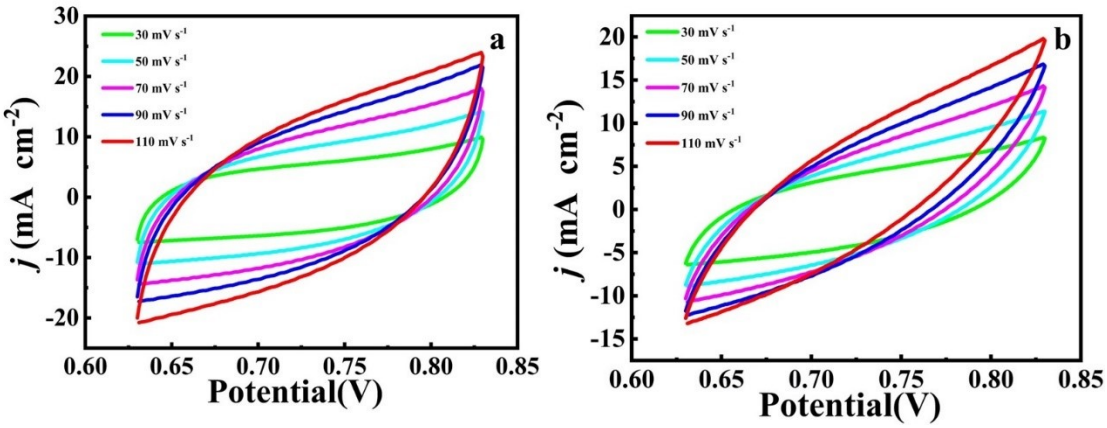

Fig. S18 CV curves within a non-faradaic reaction region of 0.85~1.10 V (vs. RHE) at different scan rates toward OER for Fe-NiS@HA(a) and NiS@HA(b)

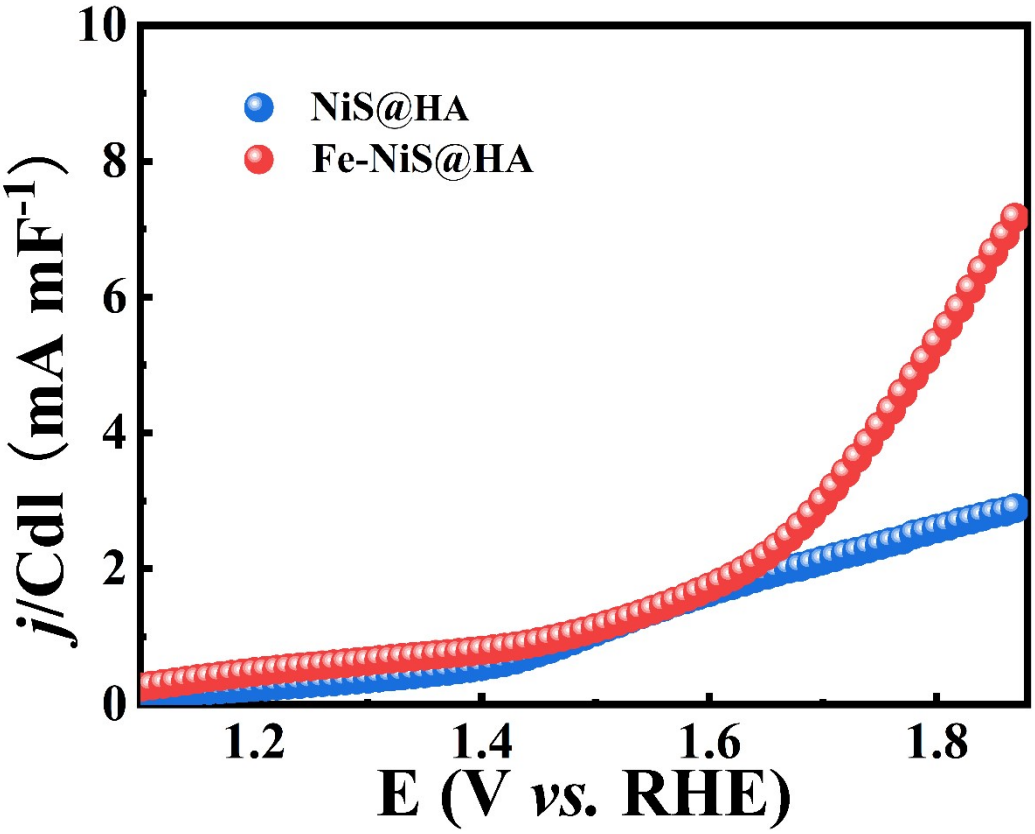

Fig. S19 C_{dl}-normalized LSV curves of Fe-NiS@HA and NiS@HA for OER.

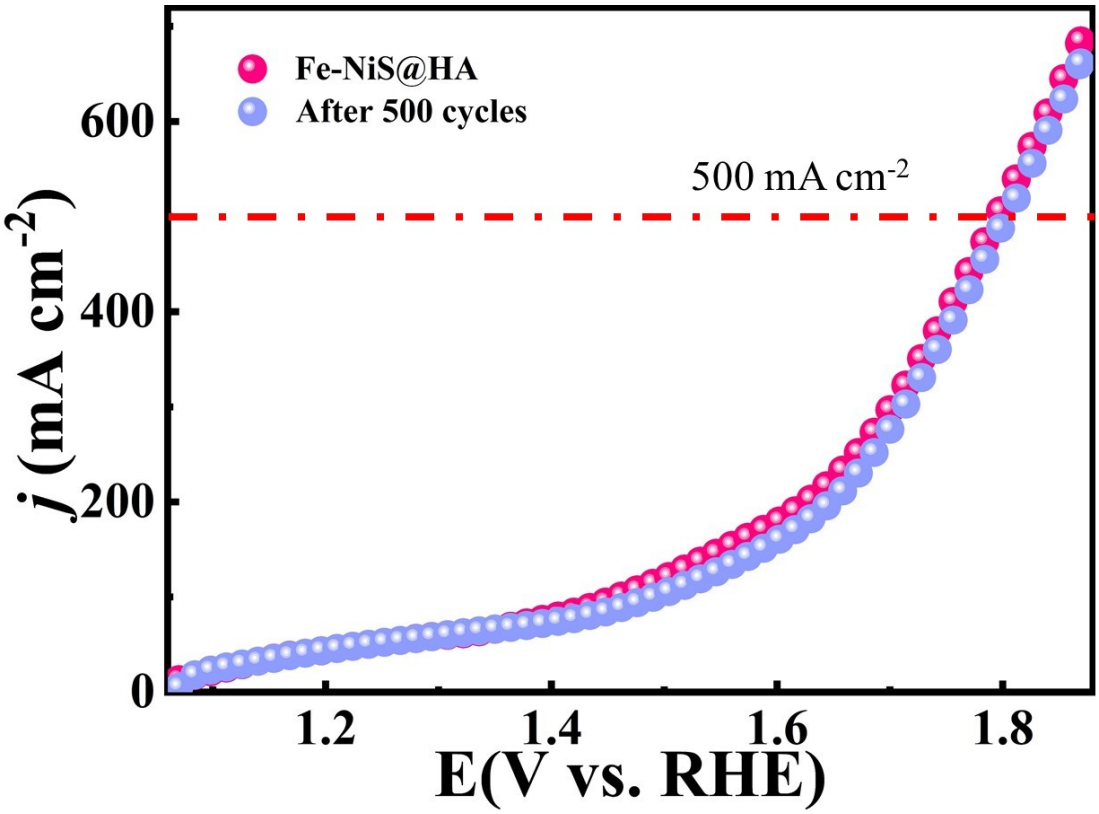

Fig. S20 LSV curves of Fe-NiS@HA before and after 500 OER cycles.

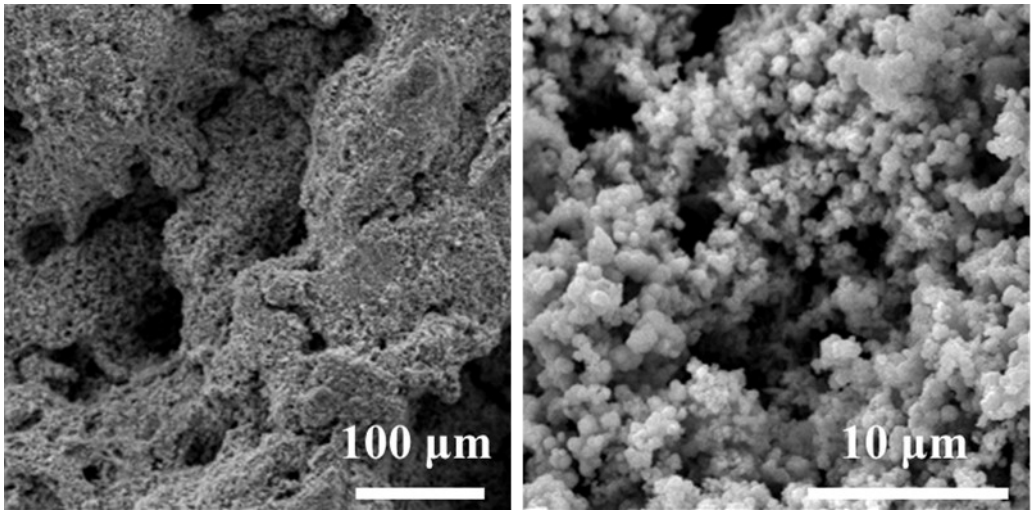

Fig. S21 SEM images of Fe-NiS@HA after OER stability test.

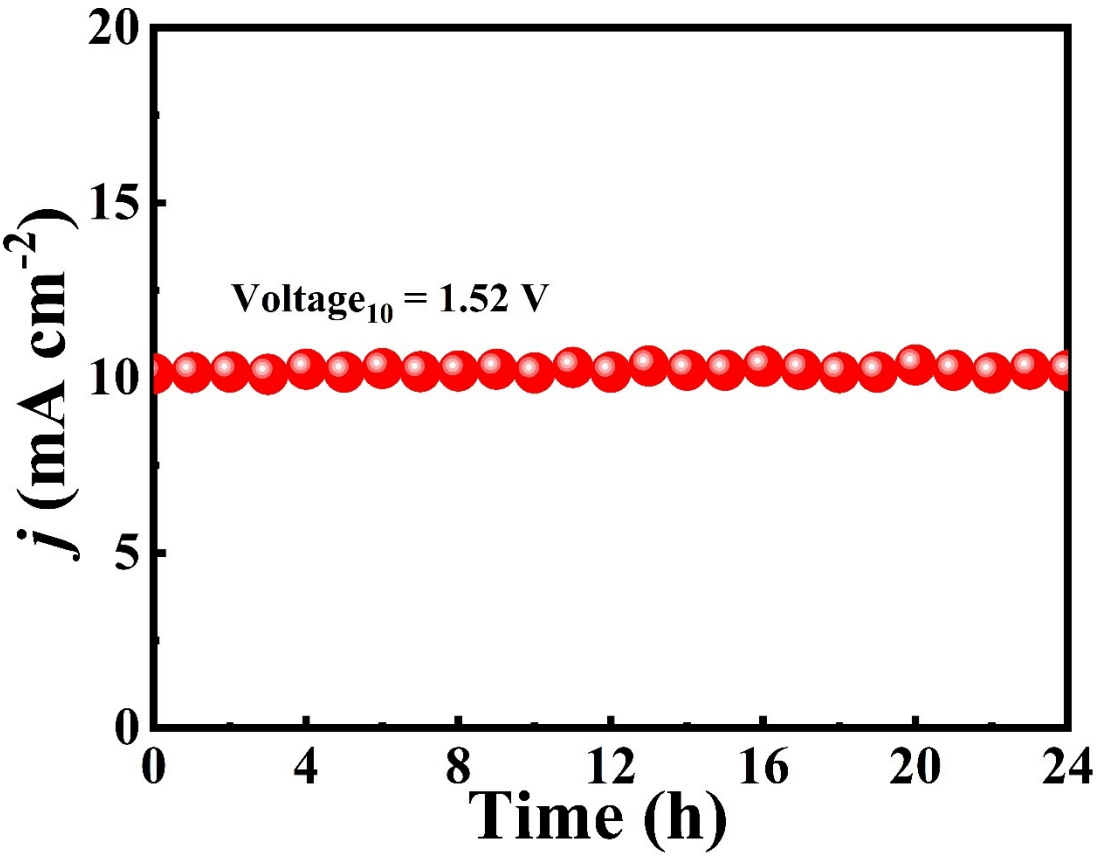

Fig. S22 Chronopotentiometry (j-t) curve of Fe-NiS@HA for overall seawater splitting at 10 mA cm^{-2}.

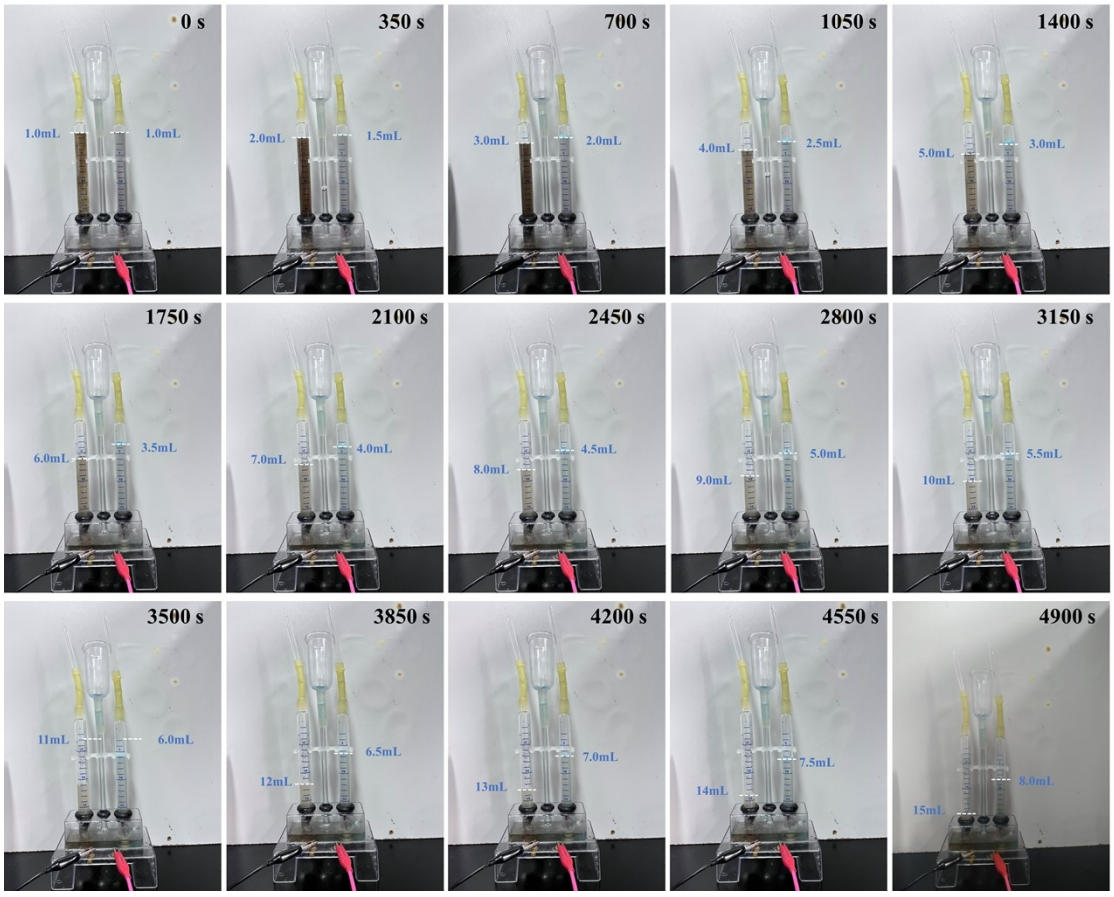

Fig. S23 The generation amount of H_2 and O_2 collected per 350 seconds at the current density of 100 mA cm^{-2}.

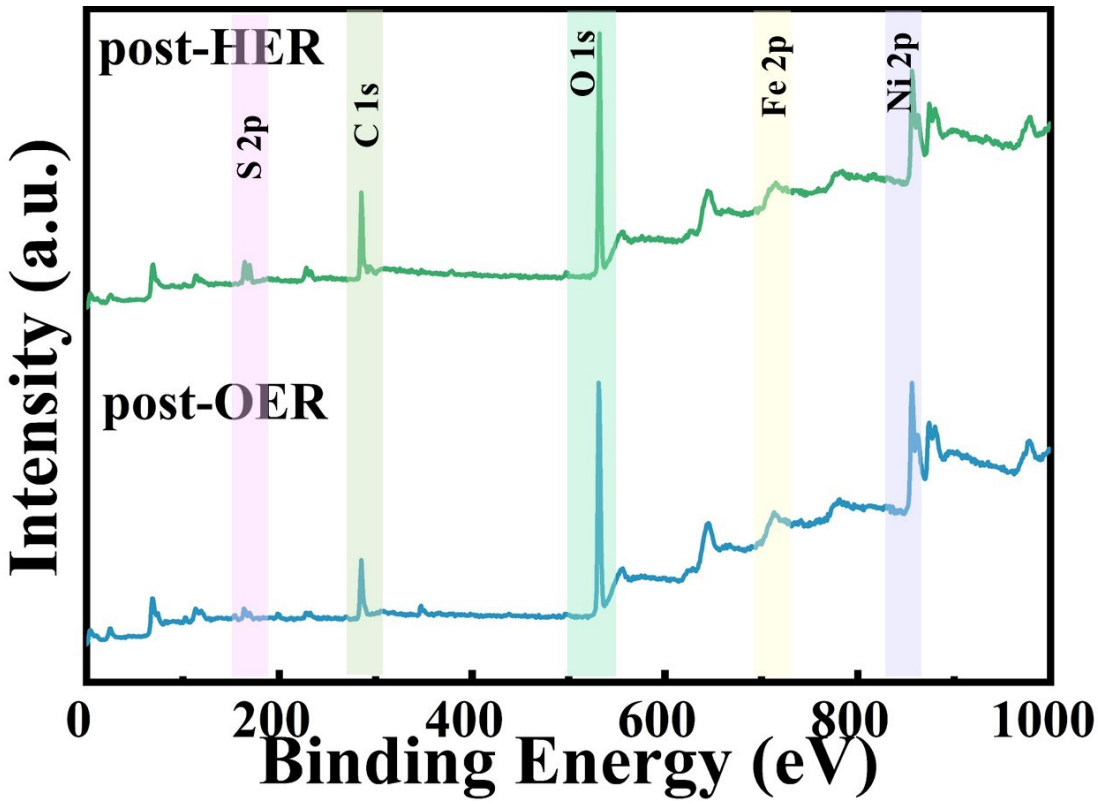

Fig. S24 High-resolution X-ray photoelectron spectroscopy spectrum for Fe-NiS@HA: (a) full spectrum, (b) Fe 2p, (c) Ni 2p, (d) S 2p and (e) O 1s.

Table S1. Comparison of HER performance of Fe-NiS@HA electrode with recently reported sulfur-based catalysts under alkaline conditions and catalysts for electrolysis of alkaline simulated seawater.

Catalyst	System	η_{10} (mV)	Tafel slope (mV/dec)	References
Fe-NiS@HA	1.0 M KOH+ 0.5 M NaCl	53	89.3	This work
S-Ni_3Se_4&Se – Ni_3S_2/NF	1.0 M KOH	89	61	[1]
S-NiFeOOH/NF	1.0 M KOH	176	90	[2]
Vs-Ni_3S_2/NF	1.0 M KOH	88	87	[3]
Ni-S-Se/NF	1.0 M KOH	98	99.4	[4]
Vs-Co_3S_4@NF	1.0 M KOH	45	66	[5]
$Ni_3Bi_2S_2$@NF	1.0 M KOH	45	53.6	[6]
Cu_8S_5/NSC-900	1.0 M KOH	137	136.8	[7]
S-RuP@NPSC	1.0 M KOH	92	90.23	[8]
Ag500-MoS2@Ni3S2/NF	1.0 M KOH	33	41.7	[9]
Co@MoS_2–S_V	1.0 M KOH	36	33	[10]
AQS/S	1.0 M KOH	62	52	[11]
CeO_2/CoS_2/Ti	1.0 M KOH	36	38	[12]
NiCoSe|S/BP	1.0 M KOH	172	128	[13]
CoSA/N,S-HCS	1.0 M KOH	165	95.6	[14]
P-Fe_3N@NC NSs/IF	1.0 M KOH	102	68.59	[15]
Ni-Sv-MoS_2	1.0 M KOH	101	66	[16]
Co_9S_8 - MoS_2/NF	1.0 M KOH	110	81.7	[17]
CoSx@Cu_2MoS_4-MoS_2/NSG	0.1 M KOH	118.1	41.1	[18]
NixSy@MnO_xH_y/NF	1.0 M KOH	179	95.1	[19]
P-NiS_2-500	1.0 M KOH	73	86.51	[20]

$Ni_3Bi_2S_2$@NF (LPTE)	1.0 M KOH	η_{100} = 127	53.6	6
Cu-NiS_2	1.0 M KOH	139	77	21
CNFMPO	1.0 M KOH+ 0.5M NaCl	73	/	22
Ni@CNTs–Mo_xC/Ni_2P	1.0 M KOH+ 0.5M NaCl	65.4	/	23
RuO_2-C-300	1.0 M KOH+ 0.5M NaCl	27	/	24
1D-Cu@Co-CoO/Rh	1.0 M KOH+ 0.5M NaCl	137.7	/	25
$Ir_{0.05}$-$Co_2P/Co_2P_2O_7$ NWs	1.0 M KOH+ 0.5M NaCl	17	/	26
Mo_x-$Ni_{0.85}Se/MoSe_2$	1.0 M KOH+ 0.5M NaCl	132	/	27

Table S2. Comparison of OER performance of Fe-NiS@HA electrode with recently reported sulfur-based catalysts under alkaline conditions and catalysts for electrolysis of alkaline simulated seawater.

Catalyst	System	η_{10} (mV)	Tafel slope (mV/dec)	References
Fe-NiS@HA	1.0 M KOH+ 0.5 M NaCl	190	92.4	This work
S-NiFeOOH/NF	1.0 M KOH	220	40	2
Vs-Co_3S_4@NF	1.0 M KOH	η_{100} = 245	60	5
$Ni_3Bi_2S_2$@NF	1.0 M KOH	127	40.9	6
Cu_8S_5/NSC-900	1.0 M KOH	313	66.5	28
A-AQS/S	1.0 M KOH	133	40	11
NiCoSe|S/BP	1.0 M KOH	285	116	13
CoSA/N,S-HCS	1.0 M KOH	306	38.1	14
P-Fe_3N@NC NSs/IF	1.0 M KOH	270	89.72	15
Co-Sv-MoS_2	1.0 M KOH	190	128	16
CoSx@Cu_2MoS_4-MoS_2/NSG	0.1 M KOH	351.4	61.5	18
NixSy@MnOxHy/NF	1.0 M KOH	η_{100} =326	39.0	19
P-NiS_2-500	1.0 M KOH	η_{100} =350	118.17	20
$Ni_3Bi_2S_2$@NF (LPTE)	1.0 M KOH	η_{100} =316	40.9	6
Cu-NiS_2	1.0 M KOH	232	46	21
Fe-Ni_3S_2	1.0 M KOH	η_{100} =290	46.9	29
Co/CoS/Fe-HSNC-700	1.0 M KOH	250	62.6	30
CCS-NiFeP-10	1.0 M KOH	201	41.2	31
Re/ReS_2-7H/CC	1.0 M KOH	290	81	32
MoS_2-AB/NF	1.0 M KOH	248	72.8	33
Ru@$MoO(S)_3$	1.0 M KOH	265	51	34

$CoFe\text{-}Ni_2P$	1.0 M KOH+ 0.5M NaCl	213	/	[35]
RuO_2-C-300	1.0 M KOH+ 0.5M NaCl	346	/	[24]
CNFMPO	1.0 M KOH+ 0.5M NaCl	282	/	[22]
$GDY/RhO_x/GDY$	1.0 M KOH+ 0.5M NaCl	193	/	[36]
Ag/NiFeRu LDH	1.0 M KOH+ 0.5M NaCl	203	/	[37]
Ni@CNTs–Mo_xC/Ni_2P	1.0 M KOH+ 0.5M NaCl	220	/	[23]

Table S3. Comparison of OWS performance of Fe-NiS@HA electrode with recently reported sulfur-based catalysts under alkaline conditions and catalysts for electrolysis of alkaline simulated seawater.

Catalyst	System	$Voltage_{10}$ (V)	References
FeNiS@HA	1.0 M KOH+ 0.5 M NaCl	1.52	This work
AQS/S ‖ A-AQS/S	1.0 M KOH	1.43	[11]
NixSy@MnOxHy/NF	1.0 M KOH	1.53	[19]
S-NiFeP-20||S-NiFeP-10	1.0 M KOH	1.5	[31]
Re/ReS_2-7H/CC	1.0 M KOH	1.3	[32]
$CoNi_2S_4/Ni_3S_2$@NF	1.0 M KOH	1.65	[38]
$Ni_3Se_2/MoSe_x$	1.0 M KOH	1.57	[39]
NiMoS	1.0 M KOH	1.53	[40]
MoS_2/NiS/NF	1.0 M KOH	1.5	[41]
Co_3S_4@MoS_2-Ni_3S_2	1.0 M KOH	1.72(50 mA cm^{-2}	[42]
MoO_2@MoS_2@Co_9S_8	1.0 M KOH	1.62	[43]
(SFCNF)/$Co_{1-x}S$@CoN	1.0 M KOH	1.58	[44]
NiCoSe|S/BP	1.0 M KOH	1.67	[13]
P-Fe_3N@NC NSs/IF	1.0 M KOH	1.61	[15]
NixSy@MnOxHy/NF	1.0 M KOH	1.529	[19]
Ag500-MoS_2@Ni_3S_2/NF	1.0 M KOH	1.47	[9]
Cu_8S_5/NSC	1.0 M KOH	1.64	[28]
NFO-Sx/IF	1.0 M KOH	1.43	[45]
$NiSe_2/Ni_3Se_4$/NF	1.0 M KOH	1.56	[46]
$Ni_3Bi_2S_2$@NF	1.0 M KOH	1.4	[6]
Co_3O_4@Mo-Co_3S_4-Ni_3S_2/NF	1.0 M KOH	1.62	[47]

$Ir_{0.05}$-$Co_2P/Co_2P_2O_7$ NWs	1.0 M KOH+ 0.5M NaCl	1.62	[26]
CNFMPO	1.0 M KOH+ 0.5M NaCl	1.56	[22]
Mn-doped Ni_2P/Fe_2P	1.0 M KOH+ 0.5M NaCl	1.64	[48]
FMCO/NF	1.0 M KOH+ 0.5M NaCl	1.58	[49]
GDY/RhO_x/GDY	1.0 M KOH+ 0.5M NaCl	1.42	[36]
Ni@CNTs–Mo_xC/Ni_2P	1.0 M KOH+ 0.5M NaCl	1.54	[23]

References

1. T.Y. Liu, P. Diao, Z. Lin, H.L. Wang, Sulfur and selenium doped nickel chalcogenides as efficient and stable electrocatalysts for hydrogen evolution reaction: The importance of the dopant atoms in and beneath the surface, *Nano Energy*,2020, **74**, 11.

2. C. Kim, S.H. Kim, S. Lee, I. Kwon, S.H. Kim, S. Kim, C. Seok, Y.S. Park, Y. Kim, Boosting overall water splitting by incorporating sulfur into NiFe (oxy)hydroxide, *J. Energy Chem.*,2022, **64**, 364-371.

3. D. Jia, L. Han, Y. Li, W. He, C. Liu, J. Zhang, C. Chen, H. Liu, H.L. Xin, Optimizing electron density of nickel sulfide electrocatalysts through sulfur vacancy engineering for alkaline hydrogen evolution, *J Mater. Chem. A*,2020, **8**, 18207-18214.

4. N. Chen, Y.-X. Du, G. Zhang, W.-T. Lu, F.-F. Cao, Amorphous nickel sulfoselenide for efficient electrochemical urea-assisted hydrogen production in alkaline media, *Nano Energy*,2021, **81**, 105605.

5. Q. Wang, H. Xu, X. Qian, G. He, H. Chen, Sulfur vacancies engineered self-supported Co3S4 nanoflowers as an efficient bifunctional catalyst for electrochemical water splitting, *Appl. Catal. B Environ.*,2023, **322**, 122104.

6. D. Yao, W. Hao, S. Weng, M. Hou, W. Cen, G. Li, Z. Chen, Y. Li, Local Photothermal Effect Enabling Ni3Bi2S2 Nanoarray Efficient Water Electrolysis at Large Current Density, *Small*,2022, **18**, 2106868.

7. L.L. Wang, W. He, D.D. Yin, Y.R. Xie, H.L. Zhang, Q.L. Ma, W.S. Yu, Y. Yang, X.T. Dong, Achieving efficient urea electrolysis by spatial confinement effect and heterostructure, *Chem. Eng. J.*,2023, **462**,

8. X. Liu, F. Liu, J. Yu, G. Xiong, L. Zhao, Y. Sang, S. Zuo, J. Zhang, H. Liu, W. Zhou, Charge Redistribution Caused by S,P Synergistically Active Ru Endows an Ultrahigh Hydrogen Evolution Activity of S-Doped RuP Embedded in N,P,S-Doped Carbon, *Adv. Sci.*,2020, **7**, 2001526.

9. X. Tong, Y. Li, Q. Ruan, N. Pang, Y. Zhou, D. Wu, D. Xiong, S. Xu, L. Wang, P.K. Chu, Plasma Engineering of Basal Sulfur Sites on MoS2@Ni3S2 Nanorods for the Alkaline Hydrogen Evolution Reaction, *Adv. Sci.*,2022, **9**, 2104774.

10. P.A. Koudakan, C. Wei, A. Mosallanezhad, B. Liu, Y. Fang, X. Hao, Y. Qian, G. Wang, Constructing Reactive Micro-Environment in Basal Plane of MoS_2 for pH-Universal Hydrogen Evolution Catalysis, *Small*,2022, **18**, 2107974.

11. Y. Chen, Z. Yu, R. Jiang, J. Huang, Y. Hou, J. Chen, Y. Zhang, H. Zhu, B. Wang, M. Wang, 3D-Stretched Film Ni3S2 Nanosheet/Macromolecule Anthraquinone Derivative Polymers for Electrocatalytic Overall Water Splitting, *Small*,2021, **17**, 2101003.

12. J. Li, Z. Xia, Q. Xue, M. Zhang, S. Zhang, H. Xiao, Y. Ma, Y. Qu, Insights into the Interfacial Lewis Acid–Base Pairs in CeO2-Loaded CoS2 Electrocatalysts for Alkaline Hydrogen Evolution, *Small*,2021, **17**, 2103018.

13. T. Liang, S. Lenus, Y. Liu, Y. Chen, T. Sakthivel, F. Chen, F. Ma, Z. Dai, Interface and M3+/M2+ Valence Dual-Engineering on Nickel Cobalt Sulfoselenide/Black Phosphorus Heterostructure for Efficient Water Splitting Electrocatalysis, *Energy Environ. Mater.*,2023, **6**, e12332.

14. Z. Zhang, X. Zhao, S. Xi, L. Zhang, Z. Chen, Z. Zeng, M. Huang, H. Yang, B. Liu, S.J. Pennycook, P. Chen, Atomically Dispersed Cobalt Trifunctional Electrocatalysts with Tailored Coordination Environment for Flexible Rechargeable Zn–Air Battery and Self-Driven Water Splitting, *Adv. Energy Mater.*,2020, **10**, 2002896.

15. G. Li, J. Yu, W. Yu, L. Yang, X. Zhang, X. Liu, H. Liu, W. Zhou, Phosphorus-Doped Iron Nitride Nanoparticles Encapsulated by Nitrogen-Doped Carbon Nanosheets on Iron Foam In Situ Derived from

Saccharomycetes Cerevisiae for Electrocatalytic Overall Water Splitting, *Small*,2020, **16**, 2001980.
16. Y. Ma, D. Leng, X. Zhang, J. Fu, C. Pi, Y. Zheng, B. Gao, X. Li, N. Li, P.K. Chu, Y. Luo, K. Huo, Enhanced Activities in Alkaline Hydrogen and Oxygen Evolution Reactions on MoS2 Electrocatalysts by In-Plane Sulfur Defects Coupled with Transition Metal Doping, *Small*,2022, **18**, 2203173.
17. M. Kim, M.A.R. Anjum, M. Choi, H.Y. Jeong, S.H. Choi, N. Park, J.S. Lee, Covalent 0D–2D Heterostructuring of Co_9S_8–MoS_2 for Enhanced Hydrogen Evolution in All pH Electrolytes, *Adv. Funct. Mater.*,2020, **30**, 2002536.
18. D.C. Nguyen, D.T. Tran, T.L.L. Doan, D.H. Kim, N.H. Kim, J.H. Lee, Rational Design of Core@shell Structured CoSx@Cu2MoS4 Hybridized MoS2/N,S-Codoped Graphene as Advanced Electrocatalyst for Water Splitting and Zn-Air Battery, *Adv. Energy Mater.*,2020, **10**, 1903289.
19. M.Y. Wang, J.H. Zhong, Z.H. Zhu, A.M. Gao, F.Y. Yi, J.Z. Ling, J.N. Hao, D. Shu, Hollow NiCoP nanocubes derived from a Prussian blue analogue self-template for high-performance supercapacitors, *J. Alloy. Compd.*,2022, **893**, 14323.
20. S. Huang, Z. Jin, P. Ning, C. Gao, Y. Wu, X. Liu, P. Xin, Z. Chen, Y. Jiang, Z. Hu, Z. Chen, Synergistically modulating electronic structure of NiS_2 hierarchical architectures by phosphorus doping and sulfur-vacancies defect engineering enables efficient electrocatalytic water splitting, *Chem. Eng. J.*,2021, **420**, 127630.
21. K.N. Dinh, Y. Sun, Z. Pei, Z. Yuan, A. Suwardi, Q. Huang, X. Liao, Z. Wang, Y. Chen, Q. Yan, Electronic Modulation of Nickel Disulfide toward Efficient Water Electrolysis, *Small*,2020, **16**, 1905885.
22. H.M. Zhang, L.H. Zuo, Y.H. Gao, J.X. Guo, C.Z. Zhu, J. Xu, J.F. Sun, Amorphous high-entropy phosphoxides for efficient overall alkaline water/seawater splitting, *J. Mater. Sci. Technol.*,2024, **173**, 1-10.
23. J.Q. Wang, D.T. Tran, K. Chang, S. Prabhakaran, J.H. Zhao, D.H. Kim, N.H. Kim, J.H. Lee, Hierarchical Ni@CNTs-bridged Mo_xC/Ni_2P heterostructure micro-pillars for enhanced seawater splitting and Mg/seawater battery, *Nano Energy*,2023, **111**, 108440.
24. F. Fang, Y. Wang, L.W. Shen, G. Tian, D. Cahen, Y.X. Xiao, J.B. Chen, S.M. Wu, L. He, K.I. Ozoemena, M.D. Symes, X.Y. Yang, Interfacial Carbon Makes Nano-Particulate RuO₂ an Efficient, Stable, pH-Universal Catalyst for Splitting of Seawater, *Small*,2022, **18**, 2203778.
25. P.K.L. Tran, D.T. Tran, D. Malhotra, S. Prabhakaran, D. Kim, N.H. Kim, J.H. Lee, Highly Effective Freshwater and Seawater Electrolysis Enabled by Atomic Rh-Modulated Co-CoO Lateral Heterostructures, *Small*,2021, **17**, 2103826.
26. V. Hoa, M. Austeria, H.T. Dao, M. Mai, D. Kim, Dual-phase cobalt phosphide/phosphate hybrid interactions via iridium nanocluster interfacial engineering toward efficient overall seawater splitting, *Appl. Catal. B Environ.*,2023, **327**, 122467.
27. Z.M. He, C.X. Zhang, S.Q. Guo, P. Xu, Y. Ji, S.W. Luo, X. Qi, Y.D. Liu, N.Y. Cheng, S.X. Dou, Y.X. Wang, B.W. Zhang, Mo-doping heterojunction: interfacial engineering in an efficient electrocatalyst for superior simulated seawater hydrogen evolution, *Chem. Sci.*,2024, **15**, 1123-1131.
28. Y. Zhang, L. Chen, B. Yan, F. Zhang, Y. Shi, X. Guo, Regeneration of textile sludge into Cu8S5 decorated N, S self-doped interconnected porous carbon as an advanced bifunctional electrocatalyst for overall water splitting, *Chem. Eng. J.*,2023, **451**, 138497.
29. Y. Liu, S.J. Xu, X.Y. Zheng, Y.K. Lu, D. Li, D.L. Jiang, Ru-doping modulated cobalt phosphide nanoarrays as efficient electrocatalyst for hydrogen evolution rection, *J. Colloid Interface Sci.*,2022, **625**, 457-465.
30. L. Yan, H. Wang, J. Shen, J. Ning, Y. Zhong, Y. Hu, Formation of mesoporous Co/CoS/Metal-N-

C@S, N-codoped hairy carbon polyhedrons as an efficient trifunctional electrocatalyst for Zn-air batteries and water splitting, *Chem. Eng. J.*,2021, **403**, 126385.
31. S. Li, L. Wang, H. Su, A.N. Hong, Y. Wang, H. Yang, L. Ge, W. Song, J. Liu, T. Ma, X. Bu, P. Feng, Electron Redistributed S-Doped Nickel Iron Phosphides Derived from One-Step Phosphatization of MOFs for Significantly Boosting Electrochemical Water Splitting, *Adv. Funct. Mater.*,2022, **32**, 2200733.
32. Q.-Q. Pang, Z.-L. Niu, S.-S. Yi, S. Zhang, Z.-Y. Liu, X.-Z. Yue, Hydrogen-Etched Bifunctional Sulfur-Defect-Rich ReS2/CC Electrocatalyst for Highly Efficient HER and OER, *Small*,2020, **16**, 2003007.
33. L. Guo, Q. Liu, Y. Liu, Z. Chen, Y. Jiang, H. Jin, T. Zhou, J. Yang, Y. Liu, Self-supported tremella-like MoS2-AB particles on nickel foam as bifunctional electrocatalysts for overall water splitting, *Nano Energy*,2022, **92**, 106707.
34. D. Chen, R. Yu, D. Wu, H. Zhao, P. Wang, J. Zhu, P. Ji, Z. Pu, L. Chen, J. Yu, S. Mu, Anion-modulated molybdenum oxide enclosed ruthenium nano-capsules with almost the same water splitting capability in acidic and alkaline media, *Nano Energy*,2022, **100**, 107445.
35. C.Q. Huang, Q.C. Zhou, L. Yu, D.S. Duan, T.Y. Cao, S.H. Qiu, Z.Z. Wang, J. Guo, Y.X. Xie, L.P. Li, Y. Yu, Functional Bimetal Co-Modification for Boosting Large-Current-Density Seawater Electrolysis by Inhibiting Adsorption of Chloride Ions, *Adv. Energy Mater.*,2023, **13**, 2301475.
36. Y. Gao, Y.R. Xue, F. He, Y.L. Li, Controlled growth of a high selectivity interface for seawater electrolysis, *Proc. Natl. Acad. Sci. U. S. A.*,2022, **119**, 7.
37. H.Y. Chen, R.T. Gao, H.J. Chen, Y. Yang, L.M. Wu, L. Wang, Ruthenium And Silver Synergetic Regulation NiFe LDH Boosting Long-Duration Industrial Seawater Electrolysis, *Adv. Funct. Mater.*,2024, 2315674.
38. W. Dai, K. Ren, Y.-a. Zhu, Y. Pan, J. Yu, T. Lu, Flower-like $CoNi_2S_4/Ni_3S_2$ nanosheet clusters on nickel foam as bifunctional electrocatalyst for overall water splitting, *J. Alloys Compd.*,2020, **844**, 156252.
39. Y. Tian, X. Xue, Y. Gu, Z. Yang, G. Hong, C. Wang, Electrodeposition of Ni3Se2/MoSex as a bifunctional electrocatalyst towards highly-efficient overall water splitting, *Nanoscale*,2020, **12**, 23125-23133.
40. C. Wang, X. Shao, J. Pan, J. Hu, X. Xu, Redox bifunctional activities with optical gain of Ni3S2 nanosheets edged with MoS_2 for overall water splitting, *Appl. Catal. B Environ.*,2020, **268**, 118435.
41. X. Xu, W. Zhong, L. Zhang, G. Liu, Y. Du, MoS_2/NiS heterostructure grown on Nickel Foam as highly efficient bifunctional electrocatalyst for overall water splitting, *Int. J. Hydrogen Energy*,2020, **45**, 17329-17338.
42. A. Muthurasu, G.P. Ojha, M. Lee, H.Y. Kim, Zeolitic imidazolate framework derived Co3S4 hybridized MoS_2–Ni_3S_2 heterointerface for electrochemical overall water splitting reactions, *Electrochim. Acta*,2020, **334**, 135537.
43. Y. Li, C. Wang, M. Cui, J. Xiong, L. Mi, S. Chen, Heterostructured MoO2@MoS2@Co9S8 nanorods as high efficiency bifunctional electrocatalyst for overall water splitting, *Appl. Surf. Sci.*,2021, **543**, 148804.
44. D. Guo, J. Wang, L. Zhang, X.a. Chen, Z. Wan, B. Xi, Strategic Atomic Layer Deposition and Electrospinning of Cobalt Sulfide/Nitride Composite as Efficient Bifunctional Electrocatalysts for Overall Water Splitting, *Small*,2020, **16**, 2002432.
45. X. Chen, Z. Qiu, H. Xing, S. Fei, J. Li, L. Ma, Y. Li, D. Liu, Sulfur-doping/leaching induced structural

transformation toward boosting electrocatalytic water splitting, *Appl. Catal. B Environ.*,2022, **305**, 121030.
46. L. Tan, J. Yu, H. Wang, H. Gao, X. Liu, L. Wang, X. She, T. Zhan, Controllable synthesis and phase-dependent catalytic performance of dual-phase nickel selenides on Ni foam for overall water splitting, *Appl. Catal. B Environ.*,2022, **303**, 120915.
47. Q. Wu, A. Dong, C. Yang, L. Ye, L. Zhao, Q. Jiang, Metal-organic framework derived Co3O4@Mo-Co3S4-Ni3S2 heterostructure supported on Ni foam for overall water splitting, *Chem. Eng. J.*,2021, **413**, 127482.
48. Y.Z. Luo, P. Wang, G.X. Zhang, S.S. Wu, Z.S. Chen, H. Ranganathan, S.H. Sun, Z.C. Shi, Mn-doped nickel-iron phosphide heterointerface nanoflowers for efficient alkaline freshwater/seawater splitting at high current densities, *Chem. Eng. J.*,2023, **454**, 140061.
49. W.X. Liu, W.B. Que, R.L. Yin, J.L. Dai, D. Zheng, J.X. Feng, X.L. Xu, F.F. Wu, W.H. Shi, X.J. Liu, X.H. Cao, Ferrum-molybdenum dual incorporated cobalt oxides as efficient bifunctional anti-corrosion electrocatalyst for seawater splitting, *Appl. Catal. B Environ.*,2023, **328**, 122488.